European Online Journal of Natural and Social Sciences 2020;
Vol.9, No 2 pp. 383-410
ISSN 1805-3602

Proteomic and Biochemical Characterisation of *F. nucleatum* Outer Membrane Vesicle

Raafat Muhammad Munshi
Department of Clinical Laboratories, King Abdulaziz University hospital, Jeddah, Saudi Arabia
Email: munshir@tcd.ie
Tel.: +966569659763

Received for publication: 23 March 2020.
Accepted for publication: 15 May 2020.

Abstract

Fusobacterium nucleatum, a gram-negative spindle-shaped anaerobic bacterium, is a component of the human microbiome that primarily inhabits the oral cavity and is associated with many diseases, including sinusitis, tonsillitis, urinary tract infection, and inflammatory bowel disease. Recent research demonstrates an association between the presence of this bacterium and colorectal carcinoma.

This study aimed to investigate the ability of this bacterium and its outer membrane vesicles (OMV) to modulate colonic cell function. Like other gram-negative bacteria, *F. nucleatum* produce OMV, but little is known about how they interact with host tissue. To investigate the potential role of these structures in the host-pathogen interaction the OMV were purified, proteomically characterised and their interaction with colonic cells investigated. In this regard, the mass spectrometry-based proteomic analysis revealed the presence of several biologically active proteases which appeared to be selectively enriched in the OMV. In addition, many other proteins with documented or likely roles in *F. nucleatum*-mediated pathogenesis were identified.

OMV impaired the barrier function of model colonic epithelial monolayers, in part by degrading the tight junctional protein (E-cadherin), which supports the hypothesis that these nanostructures likely make a significant contribution to the pathogenesis of gastrointestinal disease in susceptible individuals. However, more studies are required to identify the exact mechanisms of *F. nucleatum* OMV that associated with colorectal cancer.

Keywords: Colorectal cancer; *Fusobacterium nucleatum*; Outer membrane vesicles; Protease.

Introduction

Fusobacterium nucleatum is a gram-negative bacterium that can be isolated from a healthy and diseased individual, which associated with oral and periodontal diseases (Moore & Moore, 1994). Fusobacteria can attach to the early colonisers of dental plaque, which allow late colonisers to coadhere and involved in the growing plaque (Kaplan et al., 2014; P. E. Kolenbrander, Andersen, & Moore, 1989; Rosen, Nisimov, Helcer, & Sela, 2003). Therefore, it has been suggested that *F. nucleatum* acts as a bridging organism, which contributes to the formation of dental biofilm (P. E. Kolenbrander & London, 1993; Paul E Kolenbrander et al., 2006). Serine proteases are commonly found among proteolytic enzyme in prokaryotic and eukaryotic organisms (Page & Di Cera, 2008). Several studies report the detection of 65 kDa serine protease activity in *F. nucleatum* species (Bachrach, Rosen, Bellalou, Naor, & Sela, 2004; Doron et al., 2014; Ogawa, Brasil de Souza Tde, de Uzeda, Jankevicius, & Jankevicius, 2006). Many pathogens including Treponema denticola and *Porphyromonas gingivalis* utilises proteases to degrade host's tissue and modulate host defence sys-

tems (Abe et al., 1998; Kadowaki, Yoneda, Okamoto, Maeda, & Yamamoto, 1994). Outer membrane vesicles (OMVs) are membrane-enclosed entities of endocytic origin that produced by many microorganisms (Jan, 2017). OMV synthesised during all bacterial growth stages and mostly synthesised on stressful conditions (Kuehn & Kesty, 2005). Proteases could be found in whole bacterial cells and their outer membrane vesicles (OMVs), which may be involved in bacterial survival in the hostile host environment and in the same time inflicting damage to the host (Finlay & Falkow, 1997).

Recently, many studies are focussing on the pathogenic potential of bacterial OMV concerning how those microvesicles interact with host cells. In the past decade, there is an increase in the number of studies about OMV contribution to diseases and their use as acellular vaccines. The production of OMV considered one of the main characteristics of gram-positive and gram-negative bacteria, which are constantly discharged from the microorganism's surface in vitro and in vivo (Jun et al., 2013). Proteomic studies of OMV that based on mass spectrometry analysis of the OMV revealed the presence of a considerable amount of proteins including virulence factors and toxins (Lee, Kim, & Gho, 2016). Such studies could reveal the pathophysiological function and biogenesis of OMV. Various pathogenesis-associated molecules are incorporated into the vesicles during the production of OMV such as LPS, porins, and adhesins that mediate inflammatory response and adhesion of microorganisms and other pathogenic responses by host cells (Ellis, Leiman, & Kuehn, 2010; A. Olofsson et al., 2010). In addition, OMV is a known vector for other virulence factors including toxins (Dutta et al., 2004), and proteases (Xie, 2015). Such proteins are associated with the pathogenesis of many diseases and involved in the modulation of host immune responses. In this regard, this study aimed to characterise and identify the proteomic composition of *F. nucleatum* OMV to better understand how these structures could modulate host cellular response.

Materials and Methods

Bacterial strains and culture conditions

Three bacteria were used in the current study including *Fusobacterium nucleatum nucleatum* (ATCC 25586), *Fusobacterium nucleatum polymorphum* (ATCC 10953), and *Fusobacterium nucleatum vincentii* (ATCC 49256) were purchased from the ATCC culture collection (ATCC, LGC, UK). All microorganisms were grown at 37^{o}C under anaerobic conditions using the atmosphere generating system (AneroGen, ThermoScientific). All Fusobacteria species were thawed from frozen stock and plated on Columbia blood agar (CBA) plates (Columbia agar base, Oxoid) supplemented with 7 % v/v defibrinated horse blood. For broth culture, Fusobacteria were grown in brain heart infusion broth (BHI) which was pre-reduced for at least 24 h under anaerobic conditions before use. Different preparations of the bacteria were routinely Gram stained (Sigma) and observed microscopically under an oil immersion lens to ensure purity and to check morphology and integrity when required. The number of *F. nucleatum* was quantified as described by Gendron, Plamondon, and Grenier (2004). *F. nucleatum* were grown in BHI broth for 48 h. Before incubation with eukaryotic cells, BHI broth was removed by low-speed centrifugation and replaced with the suitable antibiotic-free medium.

Eukaryotic cell culture

The colon cancer epithelial cell lines T-84, SW-480, SW-620, and Caco-2 cells were grown at 37^{o}C and 5 % CO_2 in the appropriate medium as shown in **Table 1**. Eukaryotic cells lines and growth conditions.

Table 1. Eukaryotic cells lines and growth conditions.

Cell line	Description	Growth conditions
T-84	Human CRC adherent epithelial cells, derived from a metastatic site in the lung.	DMEM/Hams F12 medium supplemented with penicillin (100 U/ml) and streptomycin (100 µg/ml) and foetal calf serum (10 %, v/v)
SW-480	Human CRC adherent epithelial cells. Dukes stage B adenocarcinoma	RPMI medium supplemented as above
SW-620	Human CRC adherent epithelial cells. Dukes stage C adenocarcinoma	RPMI medium supplemented as above
Caco-2	human colon adenocarcinoma	EMEM medium supplemented as above with the addition of 2 mM L-glutamine.

Bacterial growth curve

Determination of the relationship between optical density (O.D) and colony forming units (CFU) is important for co-culture experiments with human cells that require usage of a specific ratio of bacteria to human cells. Typically, *F. nucleatum* was inoculated in a 25 cm^2 flask which contained 10 ml of BHI broth and incubated anaerobically as described above for 24 h at 37^oC. Then, if expansion of the culture was required, 150 µl of the bacterial suspension was subsequently inoculated into several flasks containing BHI to an OD_{600nm} of approximately 0.1. The $O.D_{600nm}$ was recorded at each time point (duplicate measurements) and 100 µl from each flask was serially diluted and spread on CBA plates followed by incubation at 37^oC for at least 72 h to allow time for individual colonies to become evident. The number of bacteria/ml was determined using the following formula:

$$\text{Number of bacteria/ml} = \frac{\text{number of CFU}}{\text{volume plated (ml)} \times \left(\frac{1}{\text{total dilution used}}\right)}$$

Recovery of the protease activity from F. nucleatum

A crude extract of cell-associated protease activity was initially obtained from *F. nucleatum* whole cells grown in BHI broth (48 h). The bacteria were pelleted by centrifugation (2087 x g, 40 min, 4^oC) and resuspended in ice-cold 25 mM Tris (pH 7.2) and subjected to sonication on ice with a Dawe Soniprep 150 at 15-20 W for 30 s (x 3) with cooling intervals. After centrifugation (2087 x g, 10 min, 4^oC) to remove intact cells and cellular debris, the resulting supernatant was passed through a 0.45 µm pore size filter (Corning Incorporated, Germany).

Proteolytic activity obtained by subculture fraction

A crude extract of the protease activity was obtained from whole cells by using different salt solutions to recover cell-surface associated protease activity. Weakly cell-surface associated or soluble protease activity was obtained by gently mixing and re-suspended *F. nucleatum* pellet in phosphate-buffered saline (PBS) prior to centrifugation (2087 x g, 40 min, 4^oC) to remove whole cells. The resulting supernatant was sterile filtered and assigned as S1 (PBS wash), and the resulting pellet was designated as P1. Stronger cell surface-associated protease activity was obtained by gently mixing P1 cells in 25 mM Tris (pH 7.2) containing 0.3 M KCL to remove additional cell surface-associated protease activity prior to centrifugation (2087 x g, 40 min, 4^oC) to remove whole cells. The resulting supernatant was sterile filtered and assigned as S2 (KCl wash), and the resulting pellet designated as P2. **Fig. 1** shows a Gram-stained image of P1, and P2 to confirm the presence of intact cells, indicating that the cells were not ruptured by the extraction procedures and that the

recovered protease activities represent material recovered from the cell surface rather than from lysed cells.

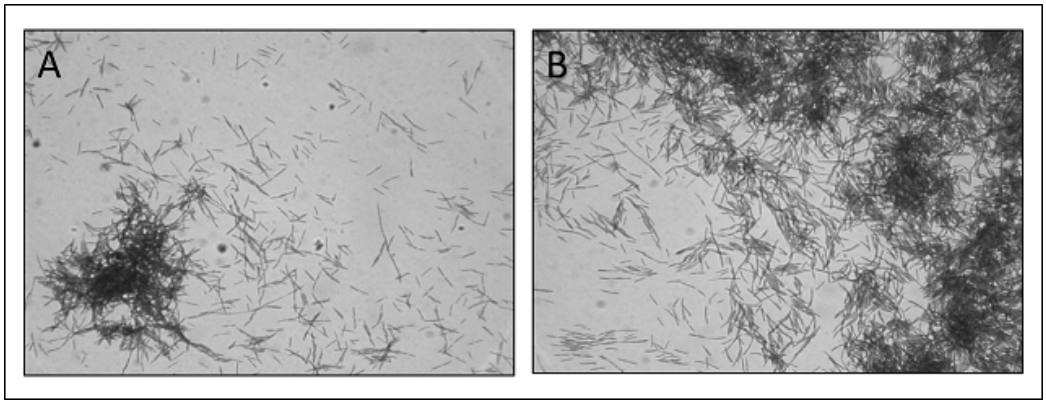

Figure 1. Gram stain of *F.* nucleatum recovered after extraction of protease activity by PBS and KCL wash. Panel A: *F. nucleatum* recovered after PBS wash, magnification (100 X). Panel B: *F. nucleatum* recovered after PBS containing 0.5 M KCl wash, magnification (100 X).

An intracellular or membrane-anchored protease activity was obtained by suspending P2 in 25 mM Tris (pH 7.2) followed by sonication as described above. The suspension was subjected to centrifugation (2087 x g, 40 min, 4^{o}C) and the supernatant subjected to a further round of centrifugation (100,000 x g, 15 min, 4^{o}C) to remove any small membrane fragments, vesicles or other cellular debris. The resulting supernatant (S3) was designated as the cytoplasmic protein fraction and the resulting pellet (P3) consisted largely of cell membranes. Finally, the membrane rich fraction (P3) was subjected to solubilisation by suspending P3 in 25 mM Tris containing 0.2 % Triton-X-100 and the resulting supernatant (S4) was considered to contain membrane bound proteins.

Protease activity assays

Proteolytic activity in crude extracts and partially purified fractions was assayed using the chromogenic substrates azocasein (casein conjugated to an azo-dye) or azoalbumin (Sulfanilic acid-azoalbumin) (Sigma, St. Louis, Mo.) essentially as described by Caldas, Cherqui, Pereira, and Simoes (2002) with minor modifications. 50 µl of sample were added to 50 µl of 2 % w/v azoalbumin in 25 mM Tris base (pH 7.2, supplemented with 0.2 M KCl, 5 mM $CaCl_2$, 1 mM $MgCl_2$ and 0.1 mM $ZnSO_4$). The mixture was then incubated at 37^{o}C for 48-72 h. Non-digested azoalbumin was precipitated by the addition of 130 µl of 10 % v/v trichloroacetic acid (TCA), incubated on ice (4^{o}C) for 30 min, and then centrifuged (1811 x g, 20 min). 100 µl of the resulting supernatant was transferred to 96-well plates containing 200 µl of 1 M NaOH and the absorbance was measured with a microplate reader (Victor) at 450 nm. Increased absorbance indicates the presence of proteolytic activity. Tris buffer (25 mM, pH 7.2) with and without KCl was treated exactly as a sample and was used as a control. Background absorbance was obtained by precipitating the substrate plus the sample in TCA without incubation.

Fractionation of the protease activities using fast protein liquid chromatography (FPLC)

Anion-exchange chromatography (Mono Q, HR 5/5) was carried out using a GE Healthcare AKTA FPLC apparatus. Bound proteins were eluted with a linear salt gradient (buffer A contained 25 mM Tris base (pH 7.2) and buffer B contained 25 mM Tris (pH 7.2) supplemented with 0.5 M KCl). Prior to FPLC, protease active material was dialyzed (BioDesignDialysis tubing) against 25 mM Tris buffer (pH 7.2) using standard procedures to remove salt. Samples were loaded and eluted at a flow rate of 1 ml/min and 300 µl fractions were collected in 96-well plates.

F. nucleatum OMV recovery

F. nucleatum OMVs were recovered essentially, as described by Mullaney et al. (2009) with slight modification. *F. nucleatum* was grown in BHI medium under the anaerobic condition at 37^{o}C in, typically, 10 x T-75 flasks, with each flask containing 50 ml of pre-reduced BHI. After 48 h of growth, the medium containing bacteria was transferred to 50 ml tubes and the bacteria were pelleted by centrifugation (2087 x g, 40 min, 4^{o}C). The resulting supernatant was filtered through a 0.45 µm filter. Following filtration, the supernatant was made 39 % with ammonium sulphate at room temperature and the mixture was incubated with stirring for 2 h at 4^{o}C prior to centrifugation (2087 x g, 40 min, 4^{o}C). The pellet containing the OMV was suspended in PBS and centrifuged (100,000 x g, 1 h, 4^{o}C) using a Sorvall Discovery SE100 ultracentrifuge. The resulting pellet was washed with PBS and centrifuged (100,000 x g, 30 min, 4^{o}C). Finally, the OMV pellet was re-suspended in 0.5 ml of PBS and stored in aliquots at -20^{o}C. Protein concentration was determined using either the BCA protein assay or a NanoDrop spectrophotometer (ND-8000).

Electron microscopy

OMV from *F. nucleatum* were subjected to electron microscopy analysis to determine purity and size heterogeneity. The OMVs were mounted onto carbon-colloidal-coated mesh grids and let settle for around 60 s. Residual non-adherent OMVs were removed using filter paper wicks. The samples were left to air dry and stained using 1 % v/v aqueous uranyl acetate prior examination by transmission electron microscopy on a Joel instrument.

Determination of protein concentration

Protein amounts were measured either by Nanodrop or by the DC or BCA protein assays (Bio-Rad), and bovine serum albumin (BSA) was used as a protein standard where required. The standard curve was constructed by serially diluting a 1 mg/ml stock and all assays were performed in triplicate.

Proteins precipitation methods

Acetone precipitation method

Ice-cold acetone was used to dilute the sample (1:5), then it was mix thoroughly and incubated at -20^{o}C for at least 2 h. The sample then centrifuged at high speed for 5 min and the supernatant was then discarded. The remaining acetone was left to evaporate at room temperature. Then, the precipitated proteins, according to the need, were re-suspended by the reducing sample buffer (ordinary gel) or non-reducing sample buffer (zymography). The proteins were then boiled at 100^{o}C for 5 min.

Trichloroacetic acid precipitation (TCA) method

One volume of 100 % w/v of TCA was added to 4 volumes of the protein sample. This was then followed by 15 min incubation at 4^{o}C. The sample then centrifuged at high speed for 5 min and the supernatant was then discarded. The precipitated proteins were suspended in the reducing sample buffer (ordinary gel) or non-reducing sample buffer (zymography). In order to bring the solution into alkaline, 0.5 µl of saturated Tris base solution was added. The proteins were then boiled at 100^{o}C for 5 min.

Sodium dodecyl sulphate polyacrylamide gel electrophoresis (SDS-PAGE)

Proteins were regularly fractionated and separated essentially as described by Laemmli (1970) using an Atto minigel apparatus (ATTO Corporation, Japan). Resolving and staking acrylamide gels prepared to the required as indicated in tables. Electrophoresis was carried out at 25 mA per gel for 1 h until the dye reached just above the gel base, at which stage electrophoresis was terminated. Two types of gels had been used throughout the experiments, both regular 12.5 % acrylamide gel **(Table 2)** or gradient gel **(Table 3)**.

Table 2. Regular gel composition.

Component	Resolving gel (12.5 %)	Stacking gel (4 %)
ddH_2O	2.5 ml	3.0 ml
Acrylamide (30 %)	3.33 ml	0.67 ml
1.5 M Tris (pH 8.8)	2 ml	-
0.5 M Tris (pH 6.8)	-	1.25 ml
10 % SDS	80 µl	50 µl
10 % Ammonium persulphate	80 µl	50 µl
TEMED	8 µl	5 µl

Table 3. Gradient gel composition.

Component	20 %	15 %	5 %	4 %
Acrylamide (30 %)	6.66 ml	5 ml	1.665 ml	1.332 ml
1.5 M Tris (pH 8.8)	2.5 ml	2.5 ml	2.5 ml	2.5 ml
water	0.785 ml	2.445 ml	5.78 ml	6.168 ml
APS (10 %)	10 µl/3ml	10 µl/3ml	10 µl/3ml	10 µl/3ml
TEMED	1 µl/3ml	1 µl/3ml	1 µl/3ml	1 µl/3ml
Sucrose	1.5 g	1.5 g	-	-
Total volume	9.95	9.95	9.95	10

SDS-PAGE for MS analysis

Colloidal Coomassie G-250 was used to stain gel when required for MS analysis. The gel was incubated for overnight in fixer (50 % v/v methanol and 2 % v/v phosphoric acid) prior to a 1 h immersion in incubation solvent (34 % v/v methanol, 2 % v/v phosphoric acid and 17 % w/v ammonium sulphate). Coomassie blue G-250 (0.25 g in 20 ml methanol) was added to the incubation solvent and left to stain for 48-72 h with gentle agitation at room temperature.

Western blotting

Western blotting was carried out essentially as described by Towbin, Staehelin, and Gordon (1979). Proteins (generally 25-50 µg/lane) were resolved typically by either by 12.5 % acrylamide or gradient acrylamide (4-15 %) SDS-PAGE gels. Proteins were transferred (1 mA/cm^2 for 1 h) to a polyvinylidene difluoride membrane (PVDF) using a semi-dry blotting apparatus (Atto). The blots were blocked with 5 % non-fat dry milk (Marvel) or 3 % BSA, in PBS, followed by probing of the membrane with the appropriate primary antibody at the recommended dilution, which then incubated for overnight at 4^oC. Blots were then washed several times with PBS containing 0.05 % v/v Tween-20, followed by incubation with the appropriate secondary antibody at the recommended dilution for 1 h at room temperature. After washing with PBS/Tween-20 antibody reactivity was visualized using enhanced chemiluminescence (ECL). Briefly, PVDF membranes were immersed for 1 min in 50 ml of Tris buffer (50 mM, pH 8.8) containing luminol (1.25 mM), iodophenol (400 µM), and hydrogen peroxide (0.01 %, v/v). Finally, the blot was exposed to Kodak X-OMAT LS film for various periods of time to capture the image; the exposed film was developed and fixed using an automated AGFA developer.

In order to interpret western blotting results, loading control was used (Tubulin for cell extracts and PCNA for nuclear fractions). This is to compensate for any different in proteins loaded in each lane. The size of each loading control band was measured by using image J software. The value

of the largest band then divided by the value of other bands which gave a factor (for each band). The resulted factors were multiplied by the size value of the corresponding sample bands.

Zymography

SDS-PAGE and Western blotting were performed using standard procedures. Zymography was performed essentially as described by T. M. Schmidt, Bleakley, and Nealson (1988) with minor modifications. Gradient (4-20 %) acrylamide gels were copolymerized with 0.05-0.1 % w/v bovine gelatin. Non-reducing sample buffer was used to solubilize samples without heat denaturation. Gels were electrophoresed at constant current (25 mA/gel). Following electrophoresis, the gels were then washed for 1 h in Triton X-100 (2.5 %, v/v) with gentle shaking, to remove excess sodium dodecyl sulphate (SDS), followed by static incubation for approximately 24 h (37^{o}C) in 25 mM Tris buffer (pH 7.2), supplemented with 5 mM $CaCl_2$). Gels were then stained with Coomassie blue (R250) for at least 1 h followed by destaining in 30 % v/v methanol and 10 % v/v acetic acid. Zones of proteolysis were visualized as clear areas against a blue background.

Mass spectrometry analysis

SDS-PAGE gel that contains proteins were excised and transferred to sterile plastic tubes. These were then subjected to in-gel digestion, using a ProGest Investigator in-gel digestion robot (Genomic Solutions, Ann Arbor, MI) using standard protocols. The analysis was undertaken by Dr. Catherine Botting (University of St Andrews, Scotland).

Transepithelial electrical resistance (TER)

Caco-2 or T-84 colonic epithelial cells were seeded on 0.4 µm filter inserts (uncoated polyethylene terephthalate plastic trace-etched membranes, Falcon, Beckton Dickinson, Oxford, United Kingdom) at a low density ($4X10^5$ cells/ml) in a 12-well plate (Falcon). The cells were fed both apically and basally every 24-48 h by changing the medium every 24-48 h. Cell confluence was assessed by phase contrast microscopy and measurement of the TER, which was measured using an EVOM epithelial voltammeter apparatus. Typically, fully polarized and differentiated monolayers took 10-14 days to form. TER measurements were taken at 24 h intervals. After the cells reached a fully polarized and differentiated state with functional tight junctions, as indicated by a stable TER reading, the monolayers were serum starved for 24 h prior to the addition of samples (bacteria cells, and OMVs). After treatment of the monolayers, the incubation was continued and the TER monitored as appropriate, as indicated in the legend to figures. The TER of monolayers without any additions represented the control for each experiment. All treatments were made either in triplicate or quadruplicate, where indicated.

Biotinylation of F. nucleatum OMVs

50 µg of OMVs were biotinylated according to the manufacturer's protocol (EZ-Link Sulfo-NHS-Biotin #21217, Thermo Scientific). Briefly, the biotin reagent (10 mM) (freshly prepared) was added to the OMV suspension and incubated at room temperature for 30 min. PBS containing 100 mM glycine was then added to the suspension, which than centrifuged (21000 x g, 2 min) at room temperature; this was repeated 3 further times with re-suspension in PBS containing 100 mM glycine each time. A Western blot (probed with streptavidin-HRP) was undertaken to ensure the OMV were biotinylated.

Fluorescence labelling of F. nucleatum OMVs

Fluorescent labelling of *F. nucleatum* OMVs was performed according to the manufacturer's protocol (Alexa Fluor 488 Protein Labelling Kit, Invitrogen). Briefly, OMVs were suspended in PBS to make a total volume of 0.5 mL, 50 µL 1 M sodium bicarbonate was then added to the OMV suspension. This solution was transferred to the Alexa Fluor 488 reactive dye vial and incubated in

the dark, with shaking for a period of 1 h. OMV were washed by ultracentrifugation to remove unreacted probe.

Immunofluorescence imaging

Following treatment and incubation of cells as required, the medium was then removed by aspiration and the cells were washed with PBS (x 2) prior to fixing the cells with 4 % paraformaldehyde (PFA) in PBS for 15 min. This was then followed by two subsequent washes with PBS. Cells were then permeabilized with 0.3 % v/v Triton X-100 in PBS for 5 min at room temperature, followed by blocking of non-specific protein binding sites with 3 % w/v bovine serum albumin (BSA) (Sigma) in PBS at room temperature for 1 h. Hoechst (nuclear stain, 1:2000) and phalloidin-TRITC (actin stain, 1:500) were added to the blocking buffer. The cells were again washed with PBS (x 2) and then incubated with primary antibody diluted in 3 % w/v BSA in PBS, using the manufacturer-specified dilution and then incubated overnight at 4^{o}C. The cells were washed then with PBS (x 3), followed by incubation with the appropriate secondary antibody (anti-mouse or anti-rabbit IgG) conjugated with Alexa 488 (Invitrogen) or Alexa 594 (Invitrogen) for 1 h at room temperature using the manufacturer-specified dilution. Cells were further washed by PBS and the cells were examined using an inverted light microscope (Nikon, Eclipse TE-300). Images were captured at different magnifications as indicated, where appropriate. Occasionally, analysis of immunofluorescence was undertaken by High Content Screening (HCS) or Confocal microscopy where indicated. HCS was performed using an InCell 1000 system. HCS images were obtained using a Nikon 10 X objective. Confocal microscopy was performed using Zeiss microscope using a 63 X objective.

Preparation of nuclear and cytoplasmic cellular extracts

Nuclear and cytoplasmic fractions of colonic epithelial cells (SW-480, SW-620, Lovo, and Caco-2) were prepared using Cytoplasmic Extraction reagent kit (Thermo Scientific, Meridian, USA). Extraction was performed according to the manufacturer's instructions. The nuclear and cytoplasmic extracts were stored at -20^{o}C until required. The protein concentration in each extract was determined by using NanoDrop spectrophotometer ND-8000.

shaken for 10 s and the florescence reading were taken at 590 nm. The statistically significant was calculated using the two-way ANOVA (Bonferroni multiple comparison).

Statistical analysis

Each experiment was carried out in triplicate or as indicated in each experiment. comparative analysis of the comparisons between the control and treatment groups using one-factor analysis of variance was carried out and the results were expressed as a mean ± SD. A student's t-test was used to determine the statistical significance using GraphPad Prism software (San Digo, CA, USA). Differences were considered significant with $P < 0.05$.

Results

Purification and mass spectrometry analysis of outer membrane vesicles recovered from F. nucleatum

As described in the methods, *F. nucleatum* OMV were visualised under transmission electron microscopy (TEM) **(Fig. 2, A)**. The recovered OMV were ranged in size from approximately 20 nm – 250 nm in diameter. The recovered OMV were free from any cellular debris as judged by TEM, then they were subjected to gradient SDS-PAGE (4 – 20 %) **(Fig. 2, B)**. This was followed by excised the gel that contained the fractionated proteins in a total of 10 pieces, as indicated in the figure. Those gel pieces were processed and analysed by mass spectrometry by Dr. Catherine Botting at the university of St. Andrew.

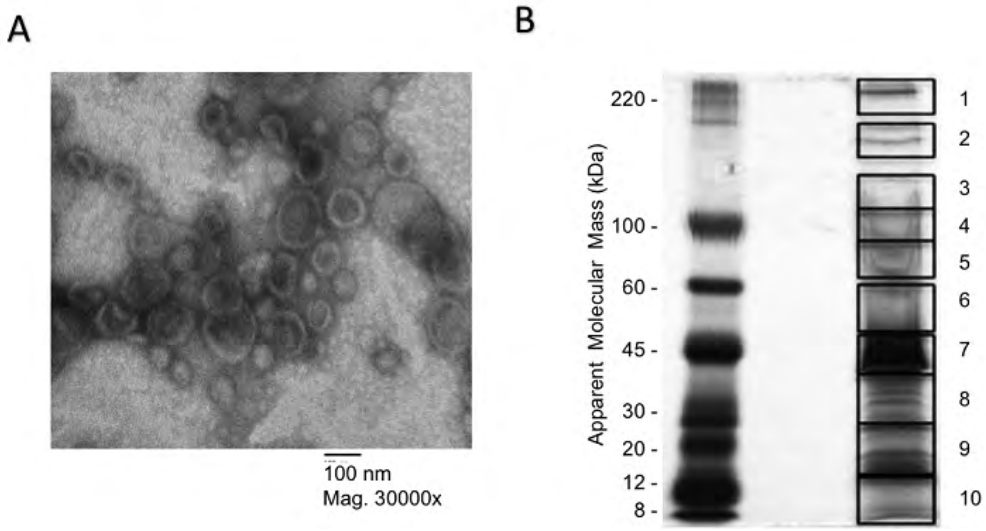

Figure 2. Transmission electron micrograph and electrophoretic analyses of OMV from *F. nucleatum*. Panel A: TEM image of purified OMV from *F. nucleatum* (magnification 30,000x; scale bar: 100 nm). Panel B: Gradient (4-20 %) SDS-PAGE analysis of *F. nucleatum* OMV. The gel lane was cut into ten separate pieces, as indicated by the boxed areas. The protein constituent in each gel piece was determined by MS analysis as described in Methods. The molecular mass markers are shown on the left-hand side.

pSORTb (v3) software tool was used for the predicted identification of the subcellular location of the putative subcellular location of the identified OMV proteins (Nancy et al., 2010). A summary of the MS-analysis result is shown in **(Fig. 3, A)**. Noticeably, the majority of the OMV-associated proteins seem to be represented by cytoplasmic proteins (50 %), whereas the rest was composed of outer membrane proteins (11 %), periplasmic proteins (4 %), cytoplasmic membrane proteins (9 %) with the balance (24 %) represented by proteins of unknown subcellular distribution. The great percentage of cytoplasmic constituents associated with *F. nucleatum* OMV is mostly due to the present of inner-outer membrane vesicles. These are characterised by the existent of both the outer and inner cytoplasmic membrane. Both double membrane (inner and outer membrane) and single membrane (outer membrane) vesicles were recovered from *F. nucleatum* **(Fig. 3, B)**.

Indeed, the identification of inner membrane proteins in the proteome supports the present of inner-outer membrane vesicles. Also, the present of inner-outer membrane vesicle provides an explanation for the high presence of cytoplasmic proteins in the proteome as these vesicles represent structures that have encapsulate cytoplasmic constituents in addition to periplasmic proteins. In previous study, 366 proteins in total were identified by the MS analysis of the OMV from *F. nucleatum* which was characterized as cytoplasmic proteins (193), cytoplasmic membrane proteins (32), periplasmic proteins (15), outer membrane proteins (37), and proteins of unknown subcellular location (89) (Munshi, 2020). As expected, the protein profile of whole bacteria and OMV were dissimilar, as identified by SDS-PAGE **(Fig. 4, A)**, that reflecting the deferential protein composition. In OMV it appears to be enrichment of high molecular mass species in compression to the whole cell whereas the distribution of low molecular mass species appears to be similar in both, but are not necessarily be the same proteins.

Mass spectrometry analysis of OMV revealed the presence of several classes of proteases (Munshi, 2020).

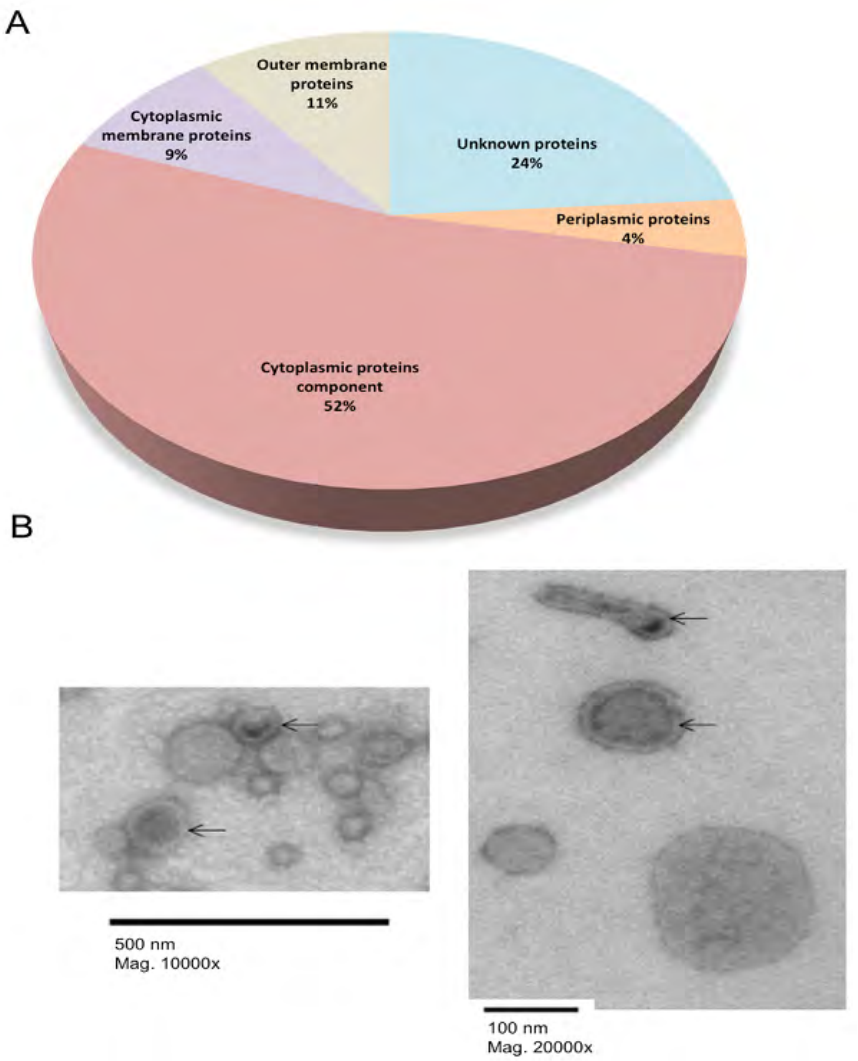

Figure 3. Mass spectrometric analysis of *F. nucleatum* OMV proteome. Panel A: Pie-chart summarising the OMV proteome. Panel B: TEM images of the OMV preparation indicating the presence of bi-layered I-OMVs (arrows). Left image magnification 10,000x; scale bar: 500 nm and right image magnification 20,000x; scale bar: 100 nm.

These incorporated proteases and peptidases whose theoretical subcellular distribution was predicted to include both cytosolic and outer membrane locations. The presence of five proteases/peptidases in the outer membrane was of particular interest given the potential for these to interact with host cells due to their predicted location on the surface of both the OMV and the intact bacteria. In order to determine whether or not these proteases were biologically active in the OMV, a preparation of OMV was subjected to analysis by zymography using gelatin as the substrate. It is clear from **(Fig. 4, B)** that there are multiple biologically active proteases associated with the OMV. Of interest was the observation that only weak proteolytic activity was found associated with the whole bacteria, at least under the conditions tested, suggesting that proteases may be differentially sorted and concentrated into OMV. There are many proteins identified in *F. nucleatum* OMV with potential virulence functions in addition to the proteases including NapA, FomA, FadA, FadD, FadI, ClpB, GroEL, and TraT.

Given the apparent abundance of proteolytic activity associated with the OMV compared to the whole cells, it was of interest to evaluate this observation further to determine if these activities could have an impact on host cells. In the first instance, attempts were made to determine and verify the subcellular distribution of the various protease activities by fractionating whole bacteria rather than OMV given the small amount of OMV available. In particular, it was of interest to identify *F. nucleatum* outer membrane-associated proteases, as these would likely interact with host cell proteins.

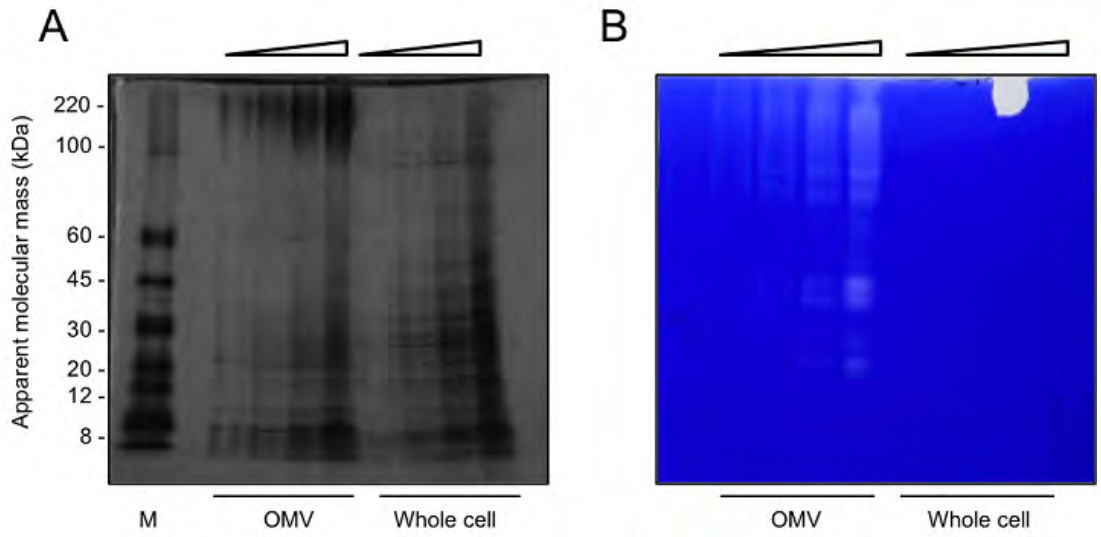

Figure 4. SDS-PAGE and zymographic analyses of OMV from *F. nucleatum*. Panel A: Gradient SDS-PAGE (4-20 %) gel loaded with increasing amounts (indicated by the gradient above the figure) of OMV and whole *F. nucleatum*. Panel B: Zymographic analysis of *F. nucleatum* whole cells and *F. nucleatum* OMV. A gradient acrylamide gel (4-20 %) containing 0.1 % gelatin was used. Zones of clearance in the zymogram indicate areas of proteolytic activity. Molecular mass markers are shown on the left-hand side.

Thus, proteins loosely associated with the bacterial surface were recovered from intact *F. nucleatum* by gently vortexing the bacteria in PBS at room temperature (fraction S1). Following centrifugation, the pellet of cells was suspended in Tris-buffer (25 mM, pH 7.4) supplemented with KCL (0.5 M) and treated similarly to extract more strongly associated cell surface proteins (fraction S2). The residual pellet was subjected to sonication followed by ultracentrifugation to recover the largely cytoplasmic proteins (fraction S3) and the membrane-bound proteins were finally recovered by solubilization of the pellet resulting from the ultracentrifugation step using 25 mM Tris containing 0.2 % v/v Triton X-100 (fraction S4) as described in the Methods section. Each fraction was subjected to SDS-PAGE **(Fig. 5, A)** and zymography **(Fig. 5, B)** to evaluate the complexity of proteins in each fraction and the subcellular distribution of proteolytic activities, respectively. Microscopic analysis of the bacteria after the PBS and KCL washes indicated that the bacteria remained intact (**Fig. 1** in the Methods section).

As the PBS extracted material appeared to contain a large proportion of the protease activity associated with whole cells **(Fig. 5, B, lane S1)** this fraction was scaled up and subjected to ion-exchange chromatography **(Fig. 6)** in an attempt to further separate the activities therein as there appeared to be multiple species present as shown by the bracket in **Fig. 5, B (lane S1)**. This indicates

that the PBS wash extracted most of the proteases found associated with the *F. nucleatum* outer membrane (loosely attached) whereas the KCL wash recovered fewer protease activities (strongly attached) **(Fig. 5, B, lane S2)**.

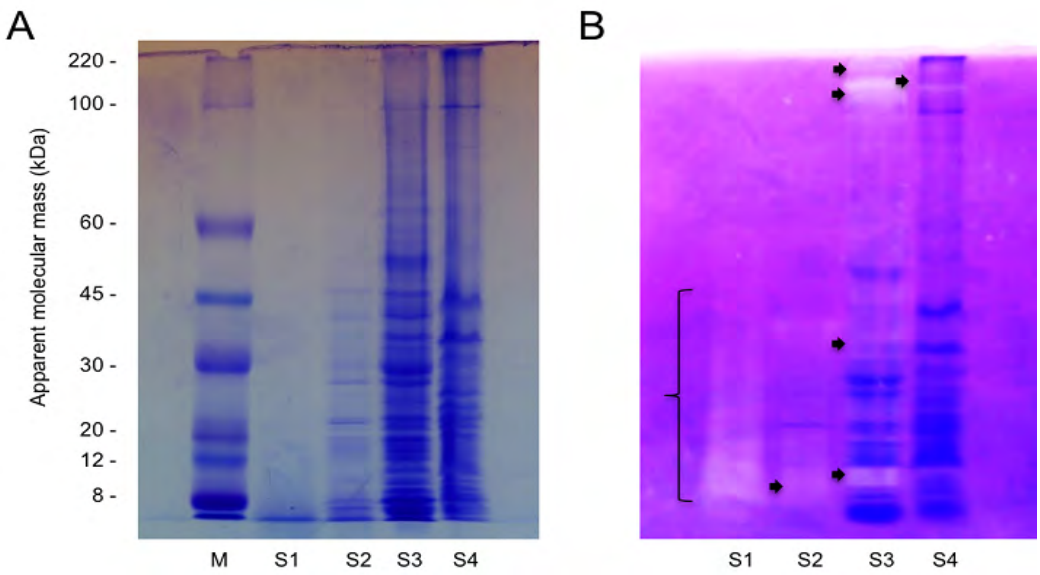

Figure 5. Subcellular fractionation of *F. nucleatum* protease activities. Fraction S1: PBS extract of whole cells. Fraction S2: 0.5 M KCL wash of PBS-treated cells. Fraction S3: cytoplasmic extract. Fraction S4 solubilized membrane extract. Panel A: Gradient SDS-PAGE (4-20 %) gel of all extracts. Panel B: Zymogram showing the protease activity present in each fraction (as indicated by arrows) using 4-20 % gradient SDS-PAGE containing 0.05 % gelatine. M= molecular size markers.

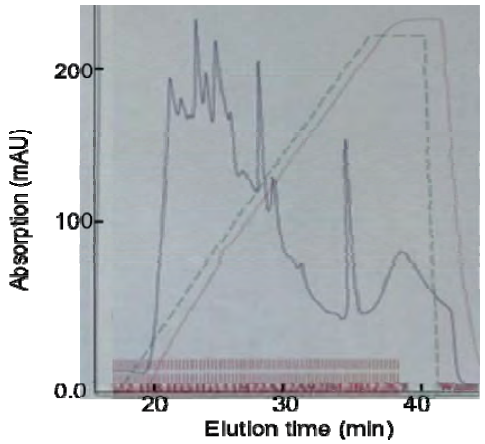

Figure 6. Ion-exchange chromatography (IEC) of PBS extract. The *F. nucleatum* PBS wash was recovered at room temperature. This was followed by dialysis against Tris (25 mM, pH 7.4). The resulting solution was subjected to ion-exchange chromatography using mono Q, HR 5/5 column and the bound proteins were eluted with a liner salt gradient (0.5 M KCL). The resulting protein fractions were collected in 96-well plates.

This fractionation was only attempted with whole bacteria, as there was insufficient biomass with a typical OMV preparation (approx. 3 mg). In an attempt to identify active fractionated protease activity, two different chromogenic protease substrates were used, azocasein and azoalbumin **(Fig. 7)**. This study revealed that the surface attached proteases exhibited differential activity towards the two substrates.

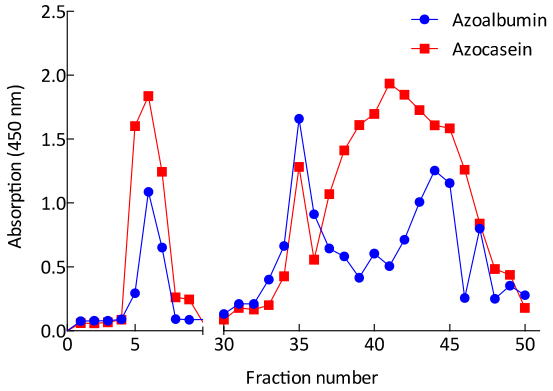

Figure 7. Analysis of the proteolytic activity obtained from *F. nucleatum* PBS wash toward azoalbumin and azocasein.

The F. nucleatum PBS wash was separated by IEC before the proteolytic activity of various fractions was tested using azoalbumin and azocasein as substrates.

Table 4. Mass spectrometry identification of proteases identified by zymography in Fig. 8, B.

Protease identified	Accession number	% Coverage	Mass	Subcellular location	Identified in OMV
Peptidase T (FN0733)	gi|19704068	18	46356	Cytoplasm	Not detected
Protease (FN1205)	gi|19704540	12	47474	Cytoplasm	Yes
Xaa-His dipeptidase (FN0278)	gi|19703623	59	50397	Cytoplasm	Yes

The PBS-extracted proteins **(Fig. 8, A)** were analyzed by SDS-PAGE **(Fig. 8, B)** which revealed the presence of multiple protein species, many of which were proteolytically active towards the gelatin **(Fig. 8, C)**. This suggests that proteases that were active against azoalbumin would not necessarily be active against gelatin as demonstrated by the lack of gelatinase activity in fraction 3 and 4.

The protein species exhibiting protease activity in fraction 15 **(Fig. 8, C)** were excised for MS-analysis from the corresponding Coomassie-stained gel as indicated by small boxes **(Fig. 8, B)**. The LC-MS/MS analysis revealed the presence of three proteolytic enzymes **(Table 4)**. Of these three proteases, two (FN1205, and FN0278) were detected previously in the MS analysis of the OMV proteome. Interestingly, pSORTb analysis of these proteins showed that they are likely to be cytosolic proteins, thus suggesting that, if truly cytosolic, they can adhere to the surface of the bacterium when present extracellularly as they were recovered from a PBS wash of intact bacteria. Phase contrast microscopy indicated that the bacteria remained intact after both the PBS and subsequent KCl washes indicating that no lysis occurred (**Fig. 1**, in the Methods section). Comparing the pro-

teolytic activities recovered from *F. nucleatum* and OMV the majority of the surface associated proteinases recovered by the PBS wash were of low molecular mass (≤ 40 kDa) whereas the proteolytic activity recovered from OMV was represented mostly by high molecular mass species (> 40 kDa).

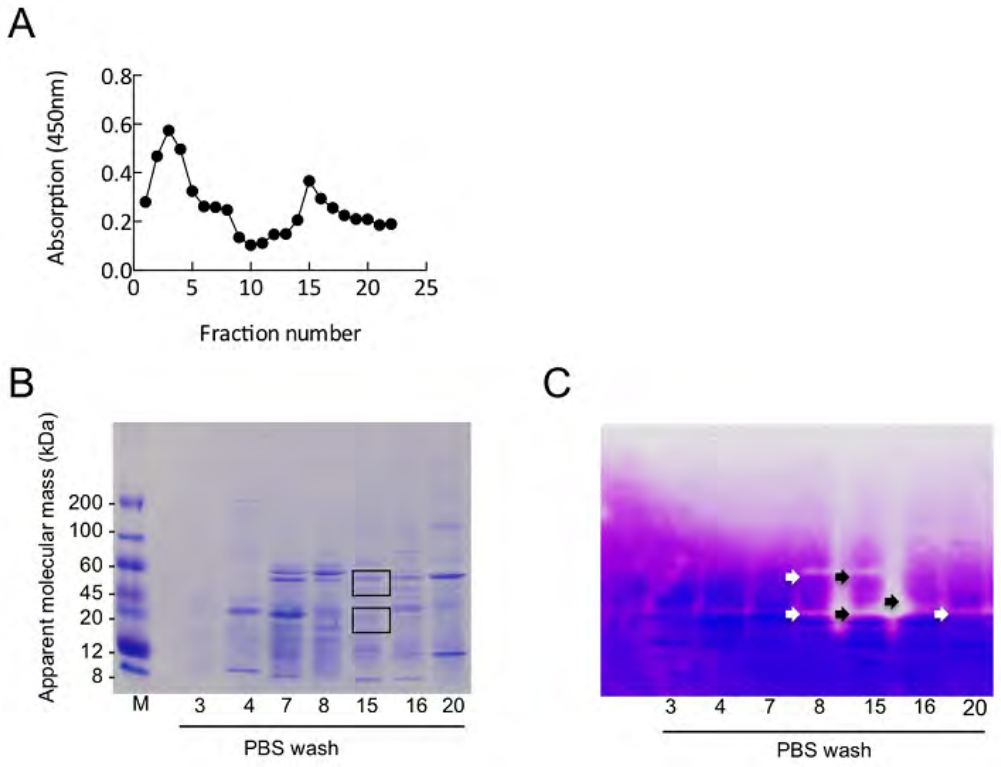

Figure 8. Analysis of the proteolytic activities obtained from *F. nucleatum* PBS wash. Panel A: Shows the proteolytic activity of the various fractions separated by IEC towards azoalbumin. Panel B: Coomassie blue stained gradient (4-20 %) acrylamide gel of the fractions indicated beneath the gel. Panel C: Zymography of the fractions shown in panel B using 4-20 % gradient SDS-PAGE containing 0.05 % gelatin. The proteolytic activity indicated by the arrows.

F. nucleatum proteases degrade host cell proteins

One study has shown that a serine protease activity recovered from *F. nucleatum* OMV was apparently able to degrade fibronectin, fibrinogen, and IgA (Bachrach et al., 2004). Thus, it was of interest to extend these studies and evaluate the ability of proteases associated with the cell surface and OMV to degrade other host proteins. In this regard, the effect of *F. nucleatum* proteolytic activity on E-cadherin, a protein involved in the maintenance of the epithelial cell barrier function, was examined **(Fig. 9)**. Recombinant human E-cadherin was incubated with *F. nucleatum* and OMV and degradation were monitored by Western blotting. Evidence of degradation was indicated by the appearance of low molecular mass peptides (56, 50.8, 42.2, 23, 19.8, and 16.4 kDa). Immunofluorescence analysis also showed a decrease in E-cadherin expression following treatment of the colonic cell line SW-480 with *F. nucleatum* and OMV **(Fig. 10)**.

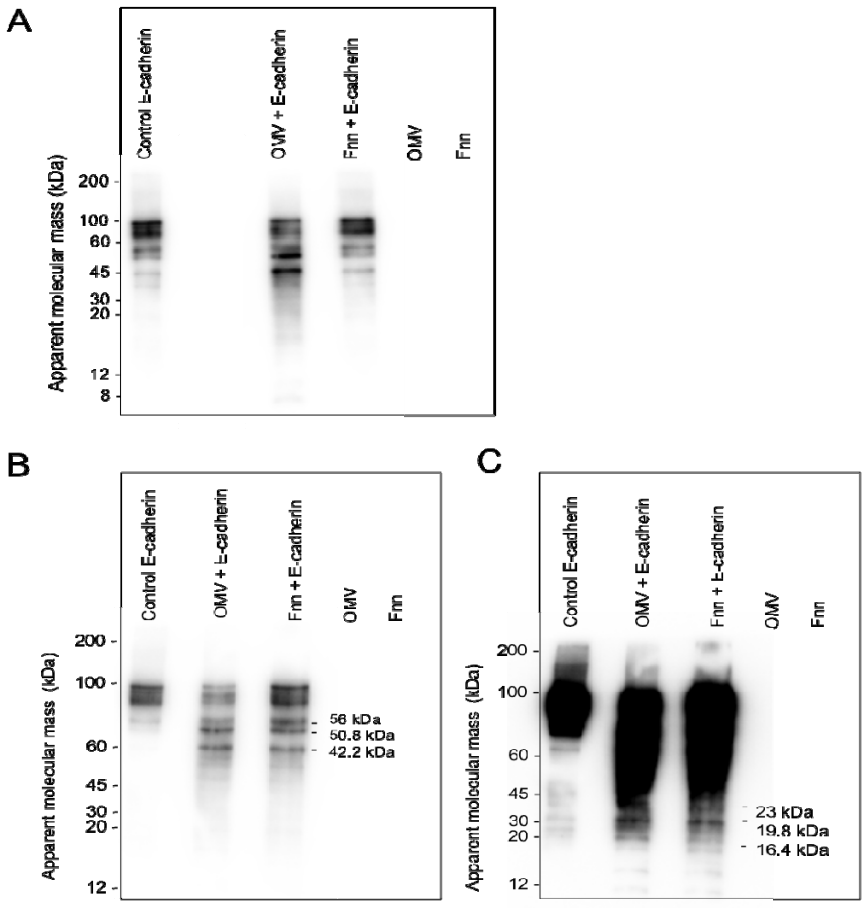

Figure 9. Effect of *F. nucleatum* and *F. nucleatum* OMVs on E-cadherin. Panel A: Purified E-cadherin was treated for 24 h with whole *F. nucleatum* (10^6 bacteria/ml) and *F. nucleatum* OMV (1.8 µg/ml). Samples were separated on 12.5 % SDS-PAGE gel, and corresponding Western Blots were probed with anti-E-cadherin. Panel B and C: Purified E-cadherin was treated for 48 h with whole *F. nucleatum* ($4.3X10^6$ bacteria/ml) and *F. nucleatum* OMV (0.59 µg/ml). Panel C shows an overexposed image of the blot shown in panel B to visualise the very low molecular mass peptides generated. Molecular mass marker are shown on the left-hand side of each panel.

Attempts were made to evaluate the ability of OMV and partially purified protease activities to degrade other host proteins including mucin, immunoglobulin (IgA), and the ECM component laminin. Under the conditions tested, degradation of mucin or IgA was not apparent (data not shown). However, evidence of degradation of laminin due to incubation with partially purified proteases from *F. nucleatum* (F5, obtained from fractionation of PBS wash by IEC) is evident due to the appearance of low molecular mass peptides when compared with the untreated protein control **(Fig. 11)**. OMV proteases also degrade laminin as indicated by the accumulation of 60 kDa material, which appears to be more intense than the corresponding band in the control sample. However, the pattern of laminin degradation by *F. nucleatum*-associated proteases activity and the OMV-associated proteases was different suggesting that the OMV harbour qualitatively different proteases activities.

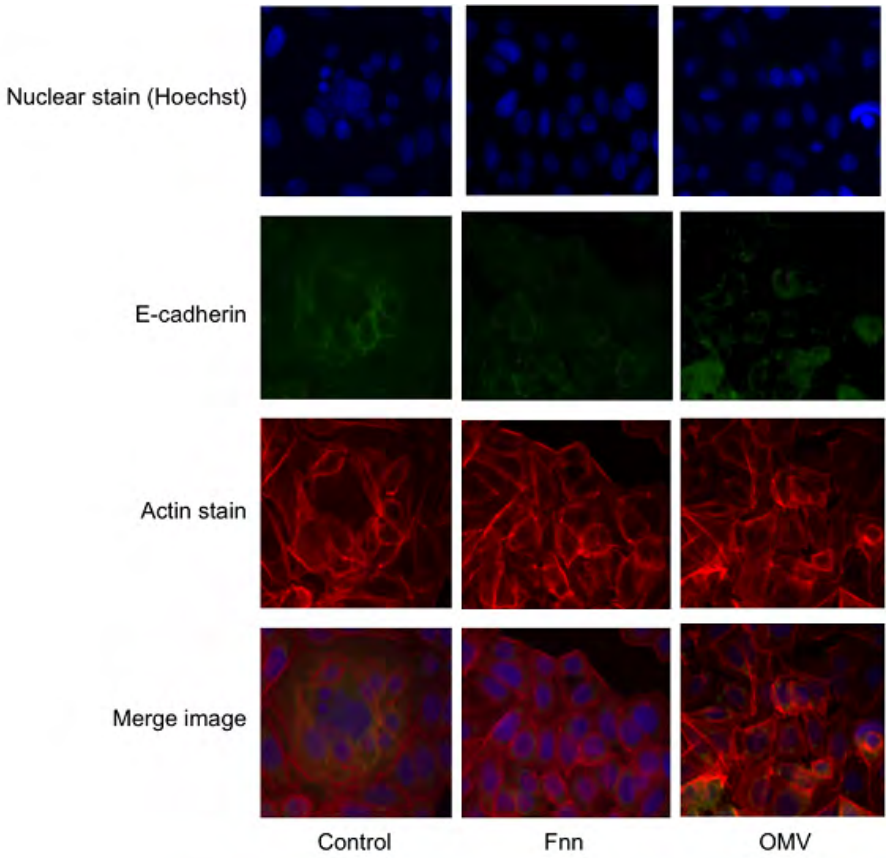

Figure 10. E-cadherin expression on SW-480 cells. SW-480 cells were treated with *F. nucleatum* (MOI 100:1) and OMV (50 µg/ml) for 24 h. SW-480 cells were washed with PBS prior to fixation and detection of E-cadherin expression by immunofluorescence (magnification 40 X).

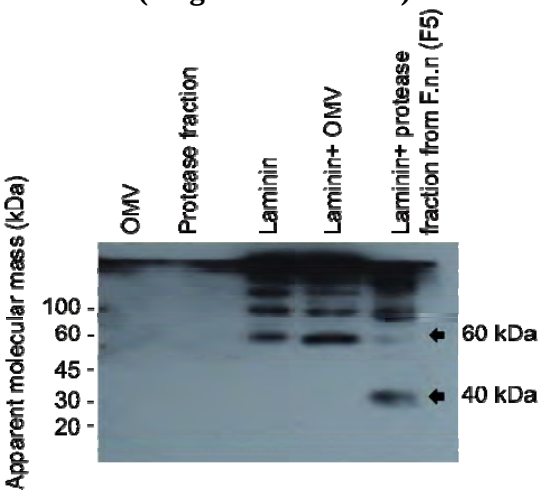

Figure 11. Effect of *F. nucleatum* OMV and partially purified proteases on laminin. Purified laminin was treated for 36 h with OMV (2 µg /ml) and F5 (a partially purified protease fraction (5 µg/ml)) obtained from a PBS wash of whole *F. nucleatum*. Samples were separated on a 12.5 % SDS-PAGE gel and laminin degradation was evaluated by Western blotting. Molecular mass markers are shown on the left-hand side.

F. nucleatum and OMV modulate epithelial barrier function of colonic epithelial cells

Given the amount of proteolytic activity associated with the OMV and their ability to degrade E-cadherin it was of interest to determine whether or not they could modulate colonic epithelial barrier function. To address this question, an in vitro model of the colonic epithelial barrier was used employing the colonic epithelial cell lines Caco-2 and T-84. Once a functional monolayer was formed in vitro, as evidenced by stable high trans-epithelial electrical resistance, the monolayer was exposed to both OMV and the intact bacterium. The data demonstrate that OMV could modulate the TER of Caco-2 monolayers in a dose-dependent manner **(Fig. 12, A)** and were more efficient than the intact bacteria in doing so. **Fig. 12, B** shows the percentage change in the TER value with time.

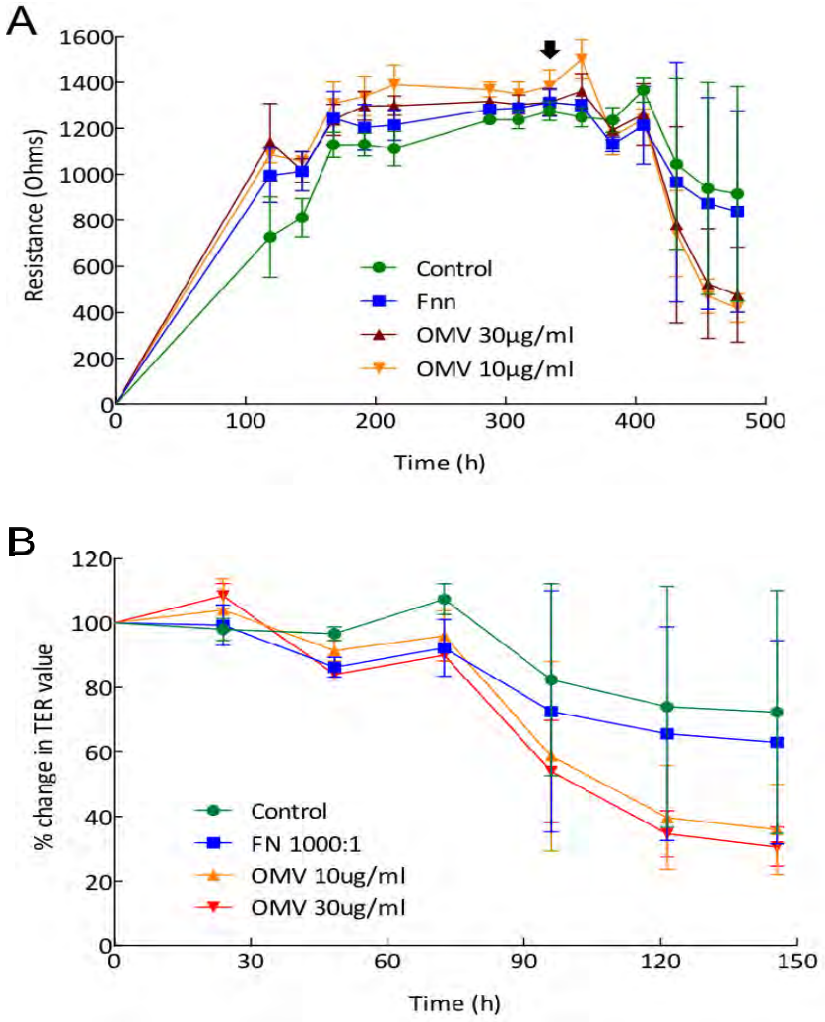

Figure 12. Effect of F. nucleatum and OMV on barrier integrity. Caco-2 cells were grown until a stable TER was achieved (approx. 13 days) and then subjected to serum deprivation for 24 h prior to sample addition. Cells were incubated with F. nucleatum (MOI 1000:1), and OMV (10 and 30 µg/ml). The results show the mean ± SEM (n=3). OMV (10 and 30 µg/ml) significantly decrease the TER ($p < 0.03$ and $p < 0.02$, respectively). Panel A: resistance value (Ohms). Panel B: the percent change in TER value after sample addition. Arrow indicates sample addition (bacterial cells and OMV).

Similarly, there was an OMV-dependent reduction in the TER across T-84 monolayers **(Fig. 13)**. Interestingly, a more rapid reduction in the TER was observed in the case of the T-84 cell model compared with the Caco-2 cell monolayer. Also, in both cases *F. nucleatum* whole cells were unable to induce a significant reduction in the TER, unlike the OMV, which could be resulted from the weakening of the whole bacterial cells due to the long exposure to atmospheric oxygen or CO_2.

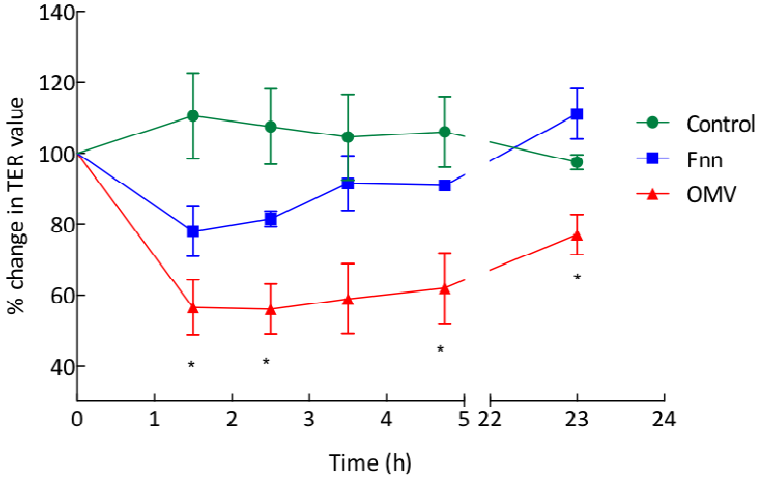

Figure 13. Effect of *F. nucleatum* and OMV on T-84 cells. T-84 cells were incubated with *F. nucleatum* (MOI 200:1), OMV (10 µg/ml). OMV significantly reduce the TER (* = P < 0.05 when compared with the same time point of the control) n=3.

Using the Caco-2 monolayer model the effect of incubating with different subspecies of *Fusobacterium* (*nucleatum*, *polymorphum*, and *vincentii*) on E-cadherin expression was evaluated. The data demonstrate that all subspecies reduced E-cadherin expression following a prolonged co-incubation (9 days) **(Fig. 14)**. Taken together, these data suggest that *F. nucleatum* OMV were able to modulate the TER, likely due to a reduction in the tight junctional protein E-cadherin.

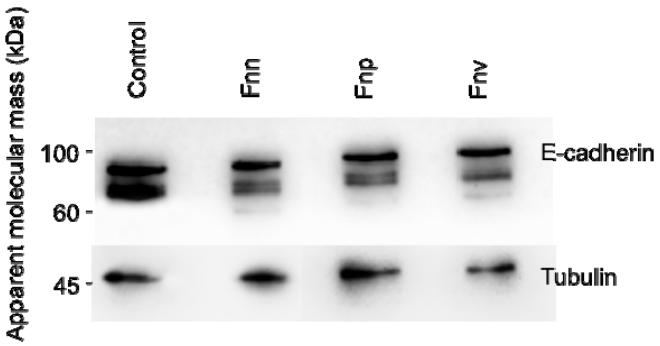

Figure 14. Effect of different *Fusobacterium* species on Caco-2 E-cadherin expression. Western blot of the lysed Caco-2 cells were probed using anti-E-cadherin after prolong exposure to Fusobacterial spices (MOI 2000:1).

Visualization of the interaction of the OMV with colonic cell lines (T-84 and SW-620) by confocal microscopy indicated that the vesicles appear to be possibly internalized by both cell lines

(Fig. 15). Also, the OMV appear to coalesce at the cell-cell boundaries as these become clearly visible when co-incubated with fluorescently labelled OMV **(Fig. 15, C)**.

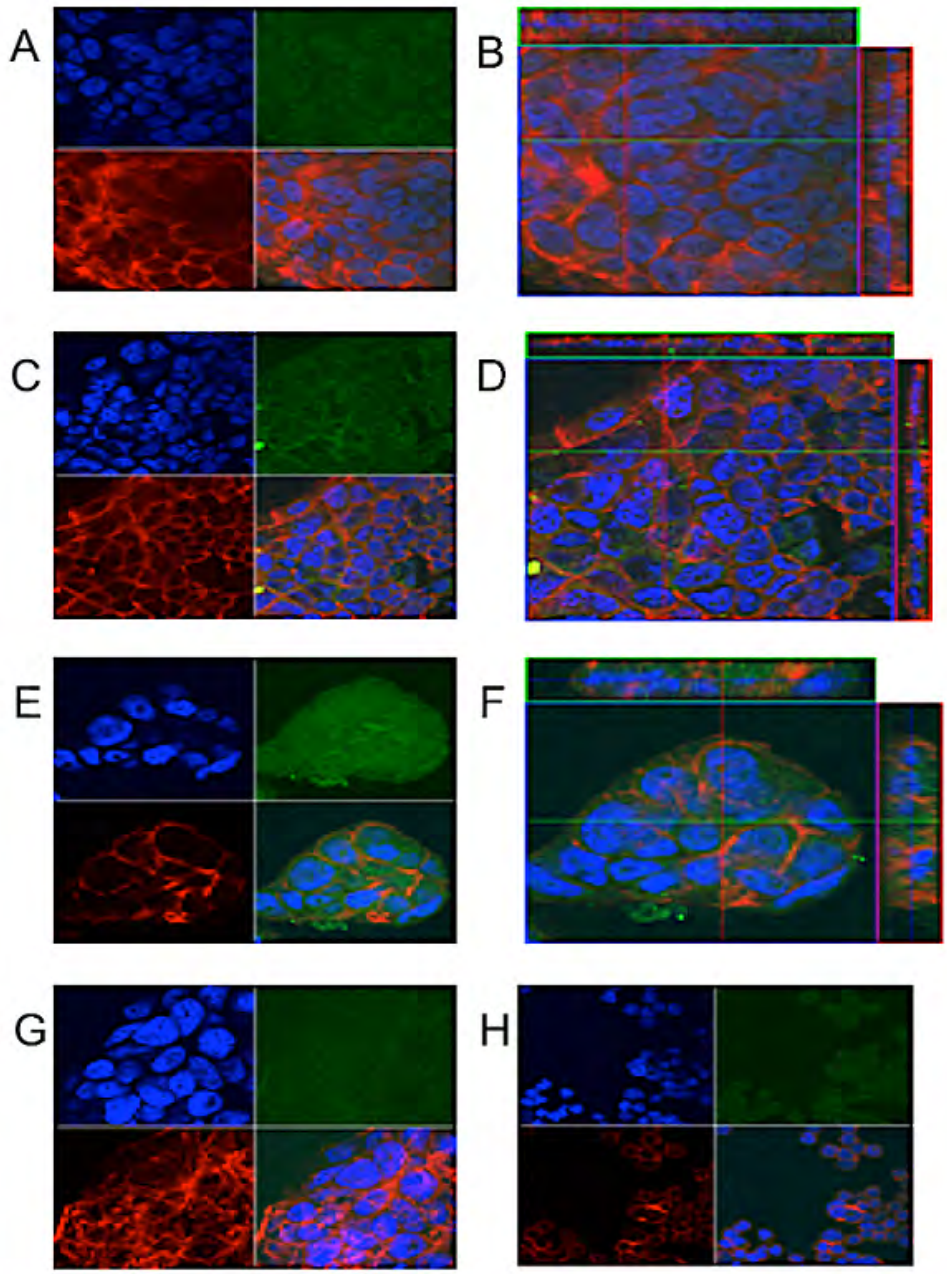

Figure 15. F. nucleatum OMV appear to bind to and be internalised by colonic epithelial cells. Panel A: T-84 cells incubated with Alexa488-OMV for 1 h; Panel B: z-stack of A; Panel C: T-84 cells incubated with Alexa488-OMV for 4 h; Panel D: z-stack of C; Panel E: T-84 cells incubated with Alexa488-OMV also for 4 h; Panel F: z-stack of E; Panel G: Control T-84 stained with phalloidin and hoechst and images captured in each channel; Panel H: SW-620 cells incubated with Alexa488-OMV for 4 h. Panels A, C, E, G and H show the individual fluorescence channels for the nuclear stain (top left quadrant), the green channel (top right quadrant), the actin stain (bottom left quadrant) and the merged image (bottom right quadrant).

Based on these observations it was hypothesised that the OMV-associated protease activity may be responsible in whole or in part for the observed effect on the TER, particularly if they could access the intracellular junctional space. To test this possibility attempts were made to inhibit protease activity with a pan-protease inhibitor cocktail. However, co-incubation of the cells with inhibitors alone resulted in a decrease in the TER (data not shown). The alternative strategy of pre-incubating the OMV with the inhibitors followed by removal of the inhibitors by ultra-centrifugal washing failed to yield useful data due in part to the fact that much of the OMV material was lost as a consequence this treatment as confirmed by SDS-PAGE (data not shown).

Discussion

This study aimed to isolate *F. nucleatum* OMV, determine the protein composition of these OMV, and undertake studies to identify potential properties of the OMV that may impact on host colonic cells. Transmission electron microscopy of the OMVs revealed the presence of two types of OMV, those with a bilayer structure and vesicles with a single membrane. Together, the MS analysis of the OMV identified 366 proteins. Interestingly, OMVs were found to be enriched in protease activity compared with the parental bacterium and the OMV-associated proteolytic activity was able to degrade the important host components E-cadherin and laminin. In addition, subcellular fractionation/purification of the loosely attached proteins indicated several proteolytic activities are associated with the surface of the bacterium. However, in this study, the protocol used to prepare the OMV involved a PBS wash prior to storing the OMV at -80^{o}C. Thus, it is most likely that the whole cell-associated proteases are washed off the surface of the OMV. This likely explains why difference are seen in the degradation pattern of laminin, for example, when treated with OMV and PBS-extracted proteases from whole *F. nucleatum*.

Many gram-negative pathogens utilize OMV as an important secretion mechanism, which enables them to deliver virulence factors into host cells at distal and local sites (Ellis & Kuehn, 2010). The vesicle structure protects multiple factors from digestion by host proteases (Kuehn & Kesty, 2005) such as protein adhesins that could facilitate invasion and transformation of the host (Renelli, Matias, Lo, & Beveridge, 2004). OMVs are important virulence factors that contribute to the pathogenicity of bacteria. For example, it has been shown that *H. pylori* OMV simulate gastric epithelial cells to produce IL-8 (Ismail, Hampton, & Keenan, 2003). *E. coli* OMV induce a lethal sepsis-like syndrome in mice that is linked to systemic induction of IL-6 and TNF-α (Park et al., 2010). Similarly, *C. jejuni* is associated with gastroenteritis and produces cytotoxic OMV capable of inducing IL-8 by intestinal epithelial cells (Elluri et al., 2014). Generally, studies such as those demonstrate that pathogenic gram-negative bacteria commonly use OMV to enhance the pathology associated with the infection.

The proteomic composition of *F. nucleatum* OMV demonstrates that they are composed of outer and inner membrane proteins, in addition to periplasmic and cytoplasmic constituents. Further, the recovery of both bilayer OMV and monolayer OMV from *F. nucleatum* raises the issue of differentiating between the functions of these vesicle types and whether they differentially interact with host cells. Curiously, some publications do not identify cytoplasmic proteins associated with OMV preparations (e.g. Sharpe, Kuehn, and Mason (2011)). A recent careful electron microscopy study concluded that the presence of a bilayer structure indicates the presence of both outer and inner membranes in populations of OMV isolated from different species of bacteria thus accounting for the presence of cytoplasmic proteins therein (Pérez-Cruz, Delgado, López-Iglesias, & Mercade, 2015). Prior to this, there was generally the mistaken assumption that OMV arose as a consequence of budding of the outer membrane alone resulting in the encapsulation of periplasmic proteins only. OMV are thus composed of outer membrane proteins, LPS, phospholipids, periplasmic proteins,

plasma membrane components, and cytoplasmic constituents (Beveridge, 1999; Pérez-Cruz et al., 2015). Cytoplasmic proteins are found in OMV from many different species including *N. meningitidis* (Lappann, Otto, Becher, & Vogel, 2013), *Francisella novicida* (Pierson et al., 2011), *H. pylori* (Mullaney et al., 2009), *A. baumannii* (Kwon, Gho, Lee, & Kim, 2009), *S. flexneri* (Chen, Liu, Fu, Wei, & Jin, 2014), *K. pneumoniae* (Cahill, Seeley, Gutel, & Ellis, 2015) and *P. aeruginosa* (Choi et al., 2011).

Recently, MS-based proteomic analysis of gram-negative OMV improved knowledge about their pathophysiological functions (Lee et al., 2016). An interesting observation arising from the MS analysis of the *F. nucleatum* OMV was the present of multiple active proteases. Microorganisms generally utilize proteases for degrading host tissues and for acquiring nutrients and have been shown to be important for survival in the host (Bamford, Fenno, Jenkinson, & Dymock, 2007). It has been shown that *F. nucleatum* may contain more than one peptidase (Rogers, Gunadi, Gully, & Zilm, 1998). The result presented in the current study, provide evidence of multiple proteolytic activities capable of using azocasein and azoalbumin as substrates. Two studies have identified a Fusobacteria serine protease (65 kDa) (Bachrach et al., 2004; Doron et al., 2014). This serine protease has been shown to be capable of inactivating host defense effectors and degrading components of periodontal tissue (Bachrach et al., 2004). OMV from different species of bacteria have been documented to contain active proteases which can be delivered to host cells tissue (Zhong, 2011). For example, proteases are preferentially and selectively packed into OMV as in case of *B. fragilis* and *B. thetaiotaomicron* (Elhenawy, Debelyy, & Feldman, 2014). Proteases interact with host cells and modulate host immune system (Rompikuntal et al., 2015), in addition to being cytotoxic, and inducing inflammatory responses (Mondal et al., 2016). Thus, proteases are considered to be important virulence factors of gram-negative bacteria in which they play a role in cytotoxicity, induction of inflammatory responses and facilitate bacterial invasion (Mondal et al., 2016).

Serine proteases are considered to be the most functionally diverse and abundant group of proteolytic enzymes in prokaryotic and eukaryotic organisms (Page & Di Cera, 2008). Extracellular secretion of serine proteases has been identified in many pathogenic gram-negative bacteria species including *Shigella, Neisseria, E. coli, Salmonella, Citrobacter rodentium, Edwardsiella* species (Ruiz-Perez & Nataro, 2014) and *V. cholerae* (Mondal et al., 2016). Possessing the ability to secrete serine proteases enables microorganisms to hydrolyze host extracellular and intracellular protein substrates, resulting in cytoskeleton destruction (Canizalez Roman & Navarro García, 2003), degradation of E-cadherin (T. P. Schmidt et al., 2016), impaired immunity (Orth et al., 2010) or induction of autophagy (Moal et al., 2011) and thus clearly have a major role in infection induced pathology.

A convenient measure of the integrity of model epithelial monolayer is to determine the TER. High TER values reflect the integrity of filter grown epithelial cells and can be used to measure perturbation of the barrier integrity. The results of this study show that only OMVs modulate the TER by decreasing the electrical resistance across polarized epithelial cells monolayers in a time-dependent manner suggesting that this barrier function is compromised. However, only the OMV induced a significant reduction in TER.

Three possibilities may account for the reduction effect on TER. Firstly, proteases associated with the OMV may participate in this process by degrading adheres junction or tight junction proteins. Efforts to inhibit the OMV-associated protease activity by using protease inhibitors were unsuccessful and resulted in de-attachment of the cells from the substratum. Alternative strategies involved pre-incubating the OMV with inhibitor then removing the inhibitors by ultracentrifugation, which was unsuccessful also due to unacceptable loss of OMV.

Secondly, the MS analysis of the OMV demonstrated that FadA is present therefore it is likely that this can bind to E-cadherin on the colonic cells. FadA is a conserved adhesin of Fusobacteria and an important virulence factor known to engage with E-cadherin and induce dissociation of β-catenin in CRC (Fardini et al., 2011; Han et al., 2005; Rubinstein et al., 2013). It has been cited by Whitmore and Lamont (2014) that gene levels of FadA in CRC is 10 time higher than normal individuals.

In support of this hypothesis, the data presented here demonstrates that OMV possibly bind to colonic cells at the cell periphery, the cellular location of E-cadherin. In addition, a consequence of this co-incubation is a decrease in the protein expression levels of E-cadherin. This latter data suggests that the observed decrease in E-cadherin expression could be responsible, in part, for the decrease seen in the TER. Thirdly, reduced E-cadherin gene expression elicited by co-incubation of colonic cell lines with *F. nucleatum* and OMV would also compromise barrier integrity as E-cadherin is functionally linked to the generation of a polarized epithelial phenotype. Any disruption to this role would likely disrupt barrier function.

The passage between the tight junctions is too narrow for bacteria to cross (Turner, 2009), and the translocation of the bacteria is a sign of impairment of intestinal integrity via tight junction pathway. EPEC decrease TER across polarized monolayers of Caco-2 by disrupting a transcellular pathway instead of disrupting intercellular tight junction (paracellular) (Canil et al., 1993). Also, It is possible that *F. nucleatum* OMVs were able to coalesce at the cell-cell boundaries, the subcellular location of E-cadherin. Several bacteria use different tactics to commandeer junctional structures for their advantage, which enables them to enter host cells. For example, *H. pylori* OMV can enter gastric cells via clathrin-dependent and independent means (Annelie Olofsson, Skalman, Obi, Lundmark, & Arnqvist, 2014). However, it appears that *F. nucleatum* enter colonic cells in a clathrin-dependent manner (Rubinstein et al., 2013).

Caco-2 and T-84 cell lines have been used as a model for studying colon cancer (Pageot et al., 2000), and intestinal epithelium development (Bernet-Camard, Coconnier, Hudault, & Servin, 1996). During active inflammation, such as in IBD, increased permeability of the epithelium can arise as a result of deterioration of the epithelial barrier function (Hollander, 1988). This contributes to pathogenesis of the disease and triggers the inflammation cascade (Sanders, 2005).

In summary, the role of *F. nucleatum* OMV in pathogenesis has not been investigated. The results presented here provide evidence of a functional role for these vesicles in modulating host cell response, but that are also distinct. It is recognized that *F. nucleatum* cause diseases, but it's emerging that OMV separately cause damage to host tissues (were efficient in degrading E-cadherin). Thus, OMV are likely important virulence factors that associate with pathogenesis and could produce damage to host cell. The MS analysis confirmed the presence of multiple proteolytic activities associated with OMV and those proteases were proteolytically active and can cause damage to host proteins. It is likely that the other immunogenic proteins identified in the OMV are also likely involved in the provocation of strong inflammatory responses, but further work is required to study these molecules further.

Acknowledgments

This work has been supported by a grant from the Ministry of Education, Saudi Arabia. Also, the author acknowledges Neal Leddy, Center for Microscopy and Analysis, TCD, for assistance with the TEM analyses.

References

Abe, N., Kadowaki, T., Okamoto, K., Nakayama, K., Ohishi, M., & Yamamoto, K. (1998). Biochemical and functional properties of lysine-specific cysteine proteinase (Lys-gingipain) as a virulence factor of Porphyromonas gingivalis in periodontal disease. Journal of biochemistry, 123(2), 305-312.

Bachrach, G., Rosen, G., Bellalou, M., Naor, R., & Sela, M. N. (2004). Identification of a Fusobacterium nucleatum 65 kDa serine protease. Mol Oral Microbiol, 19(3), 155-159. doi:10.1111/j.0902-0055.2004.00132.x

Bamford, C. V., Fenno, J. C., Jenkinson, H. F., & Dymock, D. (2007). The chymotrypsin-like protease complex of Treponema denticola ATCC 35405 mediates fibrinogen adherence and degradation. Infection and Immunntiy, 75(9), 4364-4372. doi:10.1128/IAI.00258-07

Bernet-Camard, M. F., Coconnier, M. H., Hudault, S., & Servin, A. L. (1996). Differential expression of complement proteins and regulatory decay accelerating factor in relation to differentiation of cultured human colon adenocarcinoma cell lines. Gut, 38(2), 248-253. Retrieved from https://www.ncbi.nlm.nih.gov/pubmed/8801206
http://gut.bmj.com/content/gutjnl/38/2/248.full.pdf

Beveridge, T. J. (1999). Structures of Gram-Negative Cell Walls and Their Derived Membrane Vesicles. Journal of bacteriology, 181(16), 4725-4733. Retrieved from http://jb.asm.org/content/181/16/4725.short
http://www.ncbi.nlm.nih.gov/pmc/articles/PMC93954/pdf/jb004725.pdf

Cahill, B. K., Seeley, K. W., Gutel, D., & Ellis, T. N. (2015). Klebsiella pneumoniae O antigen loss alters the outer membrane protein composition and the selective packaging of proteins into secreted outer membrane vesicles. Microbiological research, 180, 1-10. Retrieved from http://ac.els-cdn.com/S0944501315001202/1-s2.0-S0944501315001202-main.pdf?_tid=745e08a0-04b0-11e7-b890-00000aacb35e&acdnat=1489054337_b23ec2639ab045b268a2fbcf7118e488

Caldas, C., Cherqui, A., Pereira, A., & Simoes, N. (2002). Purification and characterization of an extracellular protease from Xenorhabdus nematophila involved in insect immunosuppression. Applied Environmental Microbiology, 68(3), 1297-1304. Retrieved from http://www.ncbi.nlm.nih.gov/pubmed/11872480
https://www.ncbi.nlm.nih.gov/pmc/articles/PMC123748/pdf/1302.pdf

Canil, C., Rosenshine, I., Ruschkowski, S., Donnenberg, M., Kaper, J., & Finlay, B. (1993). Enteropathogenic Escherichia coli decreases the transepithelial electrical resistance of polarized epithelial monolayers. Infect Immun, 61(7), 2755-2762. Retrieved from http://iai.asm.org/content/61/7/2755.full.pdf

Canizalez-Roman, A., & Navarro-García, F. (2003). Fodrin CaM-binding domain cleavage by Pet from enteroaggregative Escherichia coli leads to actin cytoskeletal disruption. Molecular Microbiology, 48(4), 947-958.

Chen, Y., Liu, L., Fu, H., Wei, C., & Jin, Q. (2014). Comparative proteomic analysis of outer membrane vesicles from Shigella flexneri under different culture conditions. Biochem Biophys Res Commun, 453(4), 696-702. doi:10.1016/j.bbrc.2014.09.142

Choi, D. S., Kim, D. K., Choi, S. J., Lee, J., Choi, J. P., Rho, S., . . . Gho, Y. S. (2011). Proteomic analysis of outer membrane vesicles derived from Pseudomonas aeruginosa. Proteomics, 11(16), 3424-3429. Retrieved from http://onlinelibrary.wiley.com/store/10.1002/pmic.201000212/asset/3424_ftp.pdf?v=1&t=j0290i1r&s=b761f0010a2047ea9d4d295353328bd2aedc26ba

Doron, L., Coppenhagen-Glazer, S., Ibrahim, Y., Eini, A., Naor, R., Rosen, G., & Bachrach, G. (2014). Identification and Characterization of Fusolisin, the Fusobacterium nucleatum Autotransporter Serine Protease. PLoS One, 9(10), 1-13.

Dutta, S., Iida, K. i., Takade, A., Meno, Y., Nair, G. B., & Yoshida, S. i. (2004). Release of Shiga toxin by membrane vesicles in Shigella dysenteriae serotype 1 strains and in vitro effects of antimicrobials on toxin production and release. Microbiology and Immunology, 48(12), 965-969. Retrieved from http://onlinelibrary.wiley.com/store/10.1111/j.1348-0421.2004.tb03626.x/asset/mim03626.pdf?v=1&t=j028eidd&s=13782db465307ffce23a698e1736d8179548a8b8

Elhenawy, W., Debelyy, M. O., & Feldman, M. F. (2014). Preferential packing of acidic glycosidases and proteases into Bacteroides outer membrane vesicles. mBio, 5(2), 1-14.

Ellis, T. N., & Kuehn, M. J. (2010). Virulence and immunomodulatory roles of bacterial outer membrane vesicles. Microbiology and Molecular Biology Reviews, 74(1), 81-94. doi:10.1128/MMBR.00031-09

Ellis, T. N., Leiman, S. A., & Kuehn, M. J. (2010). Naturally produced outer membrane vesicles from Pseudomonas aeruginosa elicit a potent innate immune response via combined sensing of both lipopolysaccharide and protein components. Infect Immun, 78(9), 3822-3831. doi:10.1128/IAI.00433-10

Elluri, S., Enow, C., Vdovikova, S., Rompikuntal, P. K., Dongre, M., Carlsson, S., . . . Wai, S. N. (2014). Outer membrane vesicles mediate transport of biologically active Vibrio cholerae cytolysin (VCC) from V. cholerae strains. PLoS One, 9(9), 1-13.

Fardini, Y., Wang, X., Temoin, S., Nithianantham, S., Lee, D., Shoham, M., & Han, Y. W. (2011). Fusobacterium nucleatum adhesin FadA binds vascular endothelial cadherin and alters endothelial integrity. Molecular Microbiology, 82(6), 1468-1480. doi:10.1111/j.1365-2958.2011.07905.x

Finlay, B. B., & Falkow, S. (1997). Common themes in microbial pathogenicity revisited. Microbiology and Molecular Biology Reviews, 61(2), 136-169.

Gendron, R., Plamondon, P., & Grenier, D. (2004). Binding of Pro-Matrix Metalloproteinase 9 by Fusobacterium nucleatum subsp. nucleatum as a Mechanism To Promote the Invasion of a Reconstituted Basement Membrane. Infect Immun, 72(10), 6160-6163. doi:10.1128/iai.72.10.6160-6163.2004

Han, Y. W., Ikegami, A., Rajanna, C., Kawsar, H. I., Zhou, Y., Li, M., . . . Deng, C. X. (2005). Identification and characterization of a novel adhesin unique to oral fusobacteria. Journal of bacteriology, 187(15), 5330-5340. doi:10.1128/JB.187.15.5330-5340.2005

Hollander, D. (1988). Crohn's disease--a permeability disorder of the tight junction? Gut, 29(12), 1621-1624.

Ismail, S., Hampton, M. B., & Keenan, J. I. (2003). Helicobacter pylori outer membrane vesicles modulate proliferation and interleukin-8 production by gastric epithelial cells. Infect Immun, 71(10), 5670-5675. Retrieved from https://www.ncbi.nlm.nih.gov/pubmed/14500487

Jan, A. T. (2017). Outer membrane vesicles (OMVs) of Gram-negative bacteria: a perspective update. Front Microbiol, 8, 1053.

Jun, S. H., Lee, J. H., Kim, B. R., Kim, S. I., Park, T. I., Lee, J. C., & Lee, Y. C. (2013). Acinetobacter baumannii outer membrane vesicles elicit a potent innate immune response via membrane proteins. PLoS One, 8(8), 1-8. doi:10.1371/journal.pone.0071751

Kadowaki, T., Yoneda, M., Okamoto, K., Maeda, K., & Yamamoto, K. (1994). Purification and characterization of a novel arginine-specific cysteine proteinase (argingipain) involved in the pa-

thogenesis of periodontal disease from the culture supernatant of Porphyromonas gingivalis. Journal of Biological Chemistry, 269(33), 21371-21378.

Kaplan, A., Kaplan, C. W., He, X., McHardy, I., Shi, W., & Lux, R. J. M. e. (2014). Characterization of aid1, a novel gene involved in Fusobacterium nucleatum interspecies interactions. 68(2), 379-387.

Kolenbrander, P. E., Andersen, R. N., & Moore, L. V. (1989). Coaggregation of Fusobacterium nucleatum, Selenomonas flueggei, Selenomonas infelix, Selenomonas noxia, and Selenomonas sputigena with strains from 11 genera of oral bacteria. Infect Immun, 57(10), 3194-3203. Retrieved from https://www.ncbi.nlm.nih.gov/pubmed/2777378

https://www.ncbi.nlm.nih.gov/pmc/PMC260789/

Kolenbrander, P. E., & London, J. (1993). Adhere Today, Here Tomorrow - Oral Bacterial Adherence. Journal of bacteriology, 175(11), 3247-3252. Retrieved from <Go to ISI>://WOS:A1993LE43100001

Kolenbrander, P. E., Palmer, R. J., Rickard, A. H., Jakubovics, N. S., Chalmers, N. I., & Diaz, P. I. (2006). Bacterial interactions and successions during plaque development. Periodontology 2000, 42(1), 47-79.

Kuehn, M. J., & Kesty, N. C. (2005). Bacterial outer membrane vesicles and the host-pathogen interaction. Genes & development, 19(22), 2645-2655. doi:10.1101/gad.1299905

Kwon, S.-O., Gho, Y. S., Lee, J. C., & Kim, S. I. (2009). Proteome analysis of outer membrane vesicles from a clinical Acinetobacter baumannii isolate. FEMS Microbiol Lett, 297(2), 150-156. Retrieved from http://onlinelibrary.wiley.com/store/10.1111/j.1574-6968.2009.01669.x/asset/j.1574-6968.2009.01669.x.pdf?v=1&t=j027m9ad&s=27b298a2528f8d25bf886033eeb7337ed6e827ae

Laemmli, U. K. (1970). Cleavage of structural proteins during the assembly of the head of bacteriophage T4. Nature, 227(5259), 680-685. Retrieved from https://www.ncbi.nlm.nih.gov/pubmed/5432063

Lappann, M., Otto, A., Becher, D., & Vogel, U. (2013). Comparative proteome analysis of spontaneous outer membrane vesicles and purified outer membranes of Neisseria meningitidis. Journal of bacteriology, 195(19), 4425-4435. doi:10.1128/JB.00625-13

Lee, J., Kim, O. Y., & Gho, Y. S. (2016). Proteomic profiling of Gram-negative bacterial outer membrane vesicles: Current perspectives. PROTEOMICS-Clinical Applications, 10(9-10), 897-909. doi:10.1002/prca.201600032

Moal, L. L., Comenge, Y., Ruby, V., Amsellem, R., Nicolas, V., & Servin, A. L. (2011). Secreted autotransporter toxin (Sat) triggers autophagy in epithelial cells that relies on cell detachment. Cellular microbiology, 13(7), 992-1013.

Mondal, A., Tapader, R., Chatterjee, N. S., Ghosh, A., Sinha, R., Koley, H., . . . Pal, A. (2016). Cytotoxic and Inflammatory Responses Induced by Outer Membrane Vesicle-Associated Biologically Active Proteases from Vibrio cholerae. Infect Immun, 84(5), 1478-1490. doi:10.1128/IAI.01365-15

Moore, W. E., & Moore, L. V. (1994). The bacteria of periodontal diseases. Periodontol 2000, 5(1), 66-77. Retrieved from https://www.ncbi.nlm.nih.gov/pubmed/9673163

http://onlinelibrary.wiley.com/store/10.1111/j.1600-0757.1994.tb00019.x/asset/j.1600-0757.1994.tb00019.x.pdf?v=1&t=j028tsw3&s=7242a8c0701a06e6c199b2e52c5a650dddb556f7

Mullaney, E., Brown, P. A., Smith, S. M., Botting, C. H., Yamaoka, Y. Y., Terres, A. M., . . . Windle, H. J. (2009). Proteomic and functional characterization of the outer membrane vesicles from the gastric pathogen Helicobacter pylori. Proteomic Clinical Applications, 3(7), 785-796. Retrieved from http://onlinelibrary.wiley.com/store/10.1002/prca.200800192/asset/785_ftp.pdf?v=1&t=j028zugs&s=a4e6b80d81e098d5e6c4357085ec026b9efe90e9

Munshi, R. (2020). Characterization of Outer Membrane Vesicles from Fusobacterium nucleatum. Indian Journal of Science and Technology, 13(2), 161 – 192. doi:10.17485/ijst/2020/v13i02/148492

Nancy, Y. Y., Wagner, J. R., Laird, M. R., Melli, G., Rey, S., Lo, R., . . . Foster, L. J. (2010). PSORTb 3.0: improved protein subcellular localization prediction with refined localization subcategories and predictive capabilities for all prokaryotes. Bioinformatics, 26(13), 1608-1615.

Ogawa, A. T., Brasil de Souza Tde, A., de Uzeda, M., Jankevicius, J. V., & Jankevicius, S. I. (2006). Characterization of proteolytic activities of Fusobacterium nucleatum. Journal of Endodontics, 32(6), 521-523. doi:10.1016/j.joen.2005.10.045

Olofsson, A., Skalman, L. N., Obi, I., Lundmark, R., & Arnqvist, A. (2014). Uptake of Helicobacter pylori vesicles is facilitated by clathrin-dependent and clathrin-independent endocytic pathways. mBio, 5(3), 1-14.

Olofsson, A., Vallstrom, A., Petzold, K., Tegtmeyer, N., Schleucher, J., Carlsson, S., . . . Arnqvist, A. (2010). Biochemical and functional characterization of Helicobacter pylori vesicles. Molecular Microbiology, 77(6), 1539-1555. doi:10.1111/j.1365-2958.2010.07307.x

Orth, D., Ehrlenbach, S., Brockmeyer, J., Khan, A. B., Huber, G., Karch, H., . . . Würzner, R. (2010). EspP, a serine protease of enterohemorrhagic Escherichia coli, impairs complement activation by cleaving complement factors C3/C3b and C5. Infect Immun, 78(10), 4294-4301. Retrieved from https://www.ncbi.nlm.nih.gov/pmc/articles/PMC2950363/pdf/0488-10.pdf

Page, M., & Di Cera, E. (2008). Serine peptidases: classification, structure and function. Cellular and Molecular Life Sciences, 65(7-8), 1220-1236. Retrieved from http://link.springer.com/article/10.1007%2Fs00018-008-7565-9

http://download.springer.com/static/pdf/865/art%253A10.1007%252Fs00018-008-7565-9.pdf?originUrl=http%3A%2F%2Flink.springer.com%2Farticle%2F10.1007%2Fs00018-008-7565-9&token2=exp=1489053741~acl=%2Fstatic%2Fpdf%2F865%2Fart%25253A10.1007%25252Fs00018-008-7565-9.pdf%3ForiginUrl%3Dhttp%253A%252F%252Flink.springer.com%252Farticle%252F10.1007%252Fs00018-008-7565-9*~hmac=be2e1528b46f2edf5fbf1c3ea82abb07b26460f0b1ff22ab0511b01dfab086e1

Pageot, L. P., Perreault, N., Basora, N., Francoeur, C., Magny, P., & Beaulieu, J. F. (2000). Human cell models to study small intestinal functions: Recapitulation of the crypt-villus axis. Microscopy research and technique, 49(4), 394-406. Retrieved from http://onlinelibrary.wiley.com/store/10.1002/(SICI)1097-0029(20000515)49:4%3C394::AID-JEMT8%3E3.0.CO;2-K/asset/8_ftp.pdf?v=1&t=j028et5m&s=43faf4f7b6f343e99d2f7ea06d51584efb906789

Park, K.-S., Choi, K.-H., Kim, Y.-S., Hong, B. S., Kim, O. Y., Kim, J. H., . . . Gho, Y. S. (2010). Outer membrane vesicles derived from Escherichia coli induce systemic inflammatory response syndrome. PLoS One, 5(6), 1-6.

Pérez-Cruz, C., Delgado, L., López-Iglesias, C., & Mercade, E. (2015). Outer-Inner Membrane Vesicles Naturally Secreted by Gram-Negative Pathogenic Bacteria. PLoS One, 10(1), 1-18.

Pierson, T., Matrakas, D., Taylor, Y. U., Manyam, G., Morozov, V. N., Zhou, W., & van Hoek, M. L. (2011). Proteomic characterization and functional analysis of outer membrane vesicles of Francisella novicida suggests possible role in virulence and use as a vaccine. Journal of Proteome Research, 10(3), 954-967. Retrieved from http://pubs.acs.org/doi/pdfplus/10.1021/pr1009756

Renelli, M., Matias, V., Lo, R. Y., & Beveridge, T. J. (2004). DNA-containing membrane vesicles of Pseudomonas aeruginosa PAO1 and their genetic transformation potential. Microbiology, 150(Pt 7), 2161-2169. doi:10.1099/mic.0.26841-0

Rogers, A. H., Gunadi, A., Gully, N. J., & Zilm, P. S. (1998). An aminopeptidase nutritionally important to Fusobacterium nucleatum. Microbiology, 144(7), 1807-1813. doi:10.1099/00221287-144-7-1807

Rompikuntal, P. K., Vdovikova, S., Duperthuy, M., Johnson, T. L., Åhlund, M., Lundmark, R., . . . Wai, S. N. (2015). Outer membrane vesicle-mediated export of processed PrtV protease from Vibrio cholerae. PLoS One, 10(7), 1-22. Retrieved from http://www.ncbi.nlm.nih.gov/pmc/articles/PMC4519245/pdf/pone.0134098.pdf

Rosen, G., Nisimov, I., Helcer, M., & Sela, M. N. (2003). Actinobacillus actinomycetemcomitans serotype b lipopolysaccharide mediates coaggregation with Fusobacterium nucleatum. Infect Immun, 71. doi:10.1128/iai.71.6.3652-3656.2003

Rubinstein, M. R., Wang, X., Liu, W., Hao, Y., Cai, G., & Han, Y. W. (2013). Fusobacterium nucleatum promotes colorectal carcinogenesis by modulating E-cadherin/beta-catenin signaling via its FadA adhesin. Cell Host and Microbe, 14(2), 195-206. doi:10.1016/j.chom.2013.07.012

Ruiz-Perez, F., & Nataro, J. P. (2014). Bacterial serine proteases secreted by the autotransporter pathway: classification, specificity, and role in virulence. Cell Mol Life Sci, 71(5), 745-770. doi:10.1007/s00018-013-1355-8

Sanders, D. (2005). Mucosal integrity and barrier function in the pathogenesis of early lesions in Crohn's disease. J Clin Pathol, 58(6), 568-572. Retrieved from https://www.ncbi.nlm.nih.gov/pmc/articles/PMC1770702/pdf/jcp05800568.pdf

Schmidt, T. M., Bleakley, B., & Nealson, K. H. (1988). Characterization of an Extracellular Protease from the Insect Pathogen Xenorhabdus luminescens. Applied Environmental Microbiology, 54(11), 2793-2797. Retrieved from https://www.ncbi.nlm.nih.gov/pubmed/16347777

Schmidt, T. P., Perna, A. M., Fugmann, T., Böhm, M., Hiss, J., Haller, S., . . . Rau, T. T. (2016). Identification of E-cadherin signature motifs functioning as cleavage sites for Helicobacter pylori HtrA. Scientific Reports, 6(23264), 1-12.

Sharpe, S. W., Kuehn, M. J., & Mason, K. M. (2011). Elicitation of epithelial cell-derived immune effectors by outer membrane vesicles of nontypeable Haemophilus influenzae. Infect Immun, 79(11), 4361-4369. doi:10.1128/IAI.05332-11

Towbin, H., Staehelin, T., & Gordon, J. (1979). Electrophoretic transfer of proteins from polyacrylamide gels to nitrocellulose sheets: procedure and some applications. Proc Natl Acad Sci U S A, 76(9), 4350-4354. Retrieved from https://www.ncbi.nlm.nih.gov/pmc/articles/PMC411572/pdf/pnas00009-0198.pdf

Turner, J. R. (2009). Intestinal mucosal barrier function in health and disease. Nature Reviews Immunology, 9(11), 799-809. Retrieved from http://www.nature.com/nri/journal/v9/n11/pdf/nri2653.pdf

Whitmore, S. E., & Lamont, R. J. (2014). Oral bacteria and cancer. Plos Pathogens, 10(3), 1-3.
Xie, H. (2015). Biogenesis and function of Porphyromonas gingivalis outer membrane vesicles. Future Microbiol, 10(9), 1517-1527. Retrieved from https://www.ncbi.nlm.nih.gov/pmc/articles/PMC4603655/pdf/nihms724724.pdf
Zhong, G. (2011). Chlamydia trachomatis secretion of proteases for manipulating host signaling pathways. Front Microbiol, 2, 14. doi:10.3389/fmicb.2011.00014